TM Surface-Wave Power Combining by a Planar Active-Lens Amplifier

Alfred Richard Perkons, Yongxi Qian, *Member, IEEE,* and Tatsuo Itoh, *Fellow, IEEE*

***Abstract*—Power combining of TM surface waves by a planar active-lens amplifier is the subject of this paper. An amplifier gain of 11 dB at 8.25 GHz with a 3-dB bandwidth of 0.65 GHz has been demonstrated. Gain is measured from input to output connector to facilitate comparisons with more conventional amplifiers. Measurements of output power versus input power are also presented. The amplifier behaved in a linear manner and no problems with spurious oscillations were encountered. Construction of the amplifier is compatible with planar fabrication technologies. A key component of the combiner is a microstrip-fed Yagi–Uda slot-array antenna for TM surface-wave excitation of a thick dielectric slab. Design and optimization guidelines for the antenna are presented as well as detailed spectral-domain and finite-difference time-domain (FDTD) analysis results. Measured and simulation results show an input return loss and front-to-back ratio better than 10 dB over a 5% bandwidth. Calculated and measured results for the fields radiated by the antenna confirm forward radiation of the dominant TM mode in the thick dielectric slab. Integration of the computed radiated fields shows the antenna has a surface-wave launching efficiency of 85%.**

***Index Terms*— Active antennas, active arrays, FDTD method, lens antennas, microstrip antennas, MMIC, quasi-optical amplifiers, spatial power combining, spectral-domain methods, surface waves.**

I. Introduction

QUASI-OPTICAL amplifiers have the potential for efficient power combining of large numbers of solid-state devices. Most previous work has focused on three-dimensional (3-D) approaches, such as the wave–beam type [1], grid type [2], microstrip coupling type [3], lens type [4], and waveguide-based type [5]. A quasi-optical structure based on the dielectric slab–beam waveguide (DSBW) [6] is two-dimensional (2-D) and, therefore, more amenable to planar fabrication technologies. Heat sinking of such structures should be straightforward as linear arrays of active devices are employed. An oscillator [7] and several amplifiers [8]–[11] based on the DSBW have been reported. These structures excited an electric field parallel to the slab ground plane. Such a mode has very low attenuation since the fields are zero at the ground plane and there is no conductor loss, but is difficult to excite cleanly with no perturbation or scattering loss. Dielectric lenses were used to focus and constrain the guided waves in [8]–[10]. In this paper, Yagi–Uda slot antenna arrays fed by microstrip lines are used to efficiently excite the dominant DSBW mode with the electric field normal to the slab ground plane. Microstrip delay lines are used to focus the guided waves in a manner similar to that reported in [4]. Delay-line length is analogous to thickness of a conventional dielectric lens. Commercial gain blocks are used to amplify the RF signals. Measurements of amplifier gain and output power versus input power are presented. At 8.25 GHz, an amplifier gain of 11 dB, measured from input to output connector, has been achieved [12]. The amplifier 3-dB bandwidth is 0.65 GHz.

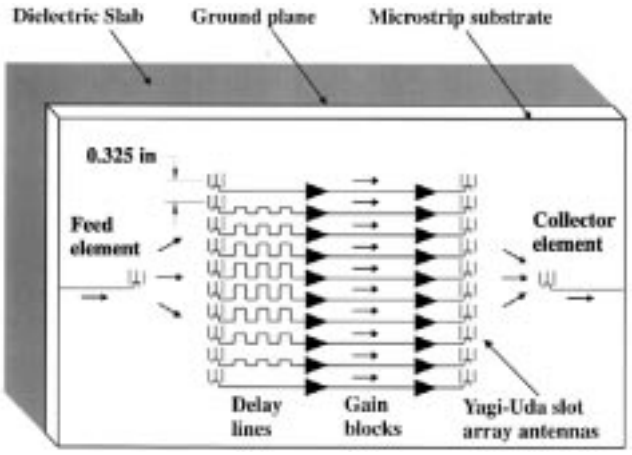

Fig. 1. A ten-element PDQ power combiner using Yagi–Uda slot-array antennas.

One of the most important components of a quasi-optical amplifier is the radiating element. Bandwidth, efficiency, mechanical robustness, and heat-sinking capability of the combiner are primarily determined by the radiating element. A microstrip-fed Yagi–Uda slot-array antenna is used to excite surface waves in a thick dielectric slab in the work reported here. The thick dielectric slab provides thermal management and mechanical support of the amplifier array. The antenna has an input return loss and front-to-back ratio better than 10 dB over a 5% bandwidth. Measured results place a lower bound of 80% on the antenna surface-wave launching efficiency. Spectral-domain simulation results predict an efficiency of 85%.

II. Design

A diagram of the planar dielectric quasi-optical (PDQ) power combiner is shown in Fig. 1. Microstrip lines and gain blocks are on the top side of a thin substrate, on top of a thick dielectric slab. Microstrip-fed Yagi–Uda slot antenna arrays on

Manuscript received October 15, 1997; revised March 4, 1998. This work was supported by the U.S. Army Research Office under Contract DAA04-94-G-0139.

The authors are with the Electrical Engineering Department, University of California, Los Angeles, Los Angeles, CA 90024 USA.

Publisher Item Identifier S 0018-9480(98)04040-X.

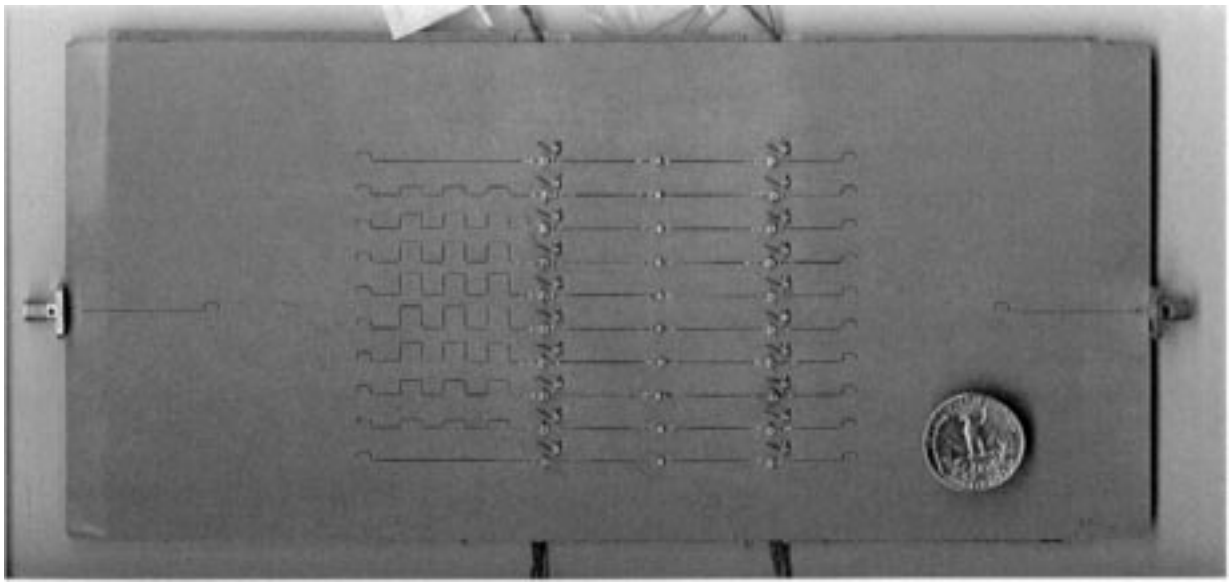

Fig. 2. Photograph of top side of PDQ power combiner.

the common ground plane are used to either receive or transmit slab–beam modes. A feed element illuminates a ten-element slab–beam active lens, which both amplifies and focuses the signal onto a collector element. Microstrip delay-line lengths are such that the total phase delay from feed to collector element is identical for each lens element. The dielectric slab and thin substrate on top of it are RT/Duroid 6010 ($\epsilon_r = 10.2, \tan\delta = 0.002$). Hewlett-Packard MGA-64 135 GaAs monolithic-microwave integrated-circuit (MMIC) amplifiers are used as the cascadable gain blocks (shown in Fig. 1). Two gain blocks cascaded together produce 18 dB of gain at 8.25 GHz. A photograph of the PDQ power combiner is shown in Fig. 2.

Heat sinking of transmission-type active antenna arrays is a difficult task [13]. Conventional 3-D quasi-optical power combiners use planar 2-D amplifier arrays. A linear amplifier array is easier to heat sink than a 2-D one. 2-D quasi-optical amplifiers employ linear amplifier arrays and are based on a thick dielectric slab. The thick dielectric slab performs three key functions: it serves as a low-loss propagation media for power combining, provides mechanical support for the thin dielectric substrate on which the active amplifier arrays are realized, and can be used to remove waste heat away from the amplifier array. 2-D quasi-optical amplifiers are inherently robust from mechanical and thermal management viewpoints.

Design of an antenna array, active or passive, begins with the selection and development of a suitable radiating element. 2-D power combiners require an efficient launcher of the desired surface-wave mode [10]. A well-designed surface-wave launcher should simultaneously satisfy the following criteria:

1) mode purity (dominant TE or TM mode);
2) high launching efficiency into the dielectric slab with good field confinement;
3) well-formed Gaussian-like transverse field profile;
4) unidirectional surface-wave radiation patterns—good front-to-back ratio;

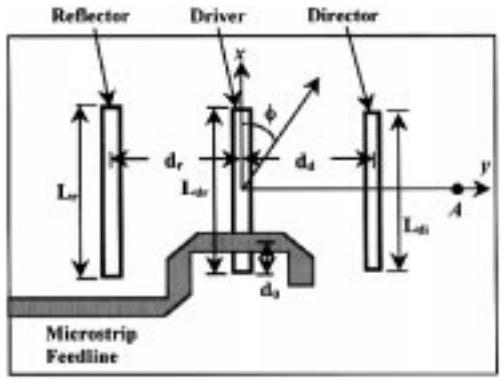

(a)

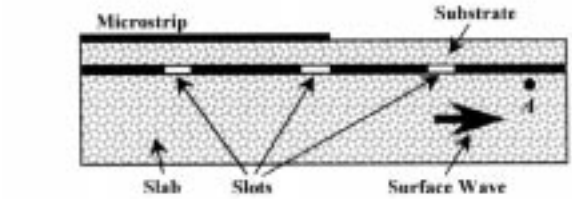

(b)

Fig. 3. (a) Top view and (b) side view of the three-element Yagi–Uda slot array for launching and receiving of TM surface waves in a dielectric slab.

5) good input match and low mutual coupling;
6) reasonable frequency bandwidth.

A Yagi–Uda slot-array antenna with one reflector and one director was selected as a candidate for efficient excitation of the dominant TM surface-wave mode in a dielectric slab. Details of the three-element Yagi–Uda slot-array antenna are shown in Fig. 3. The slots are etched on a common ground

plane separating the slab and microstrip substrates, and the driving slot is fed by a 50-Ω microstrip line on top of the thin substrate. The antenna should be designed to launch the desired dominant TM mode with a well-defined field profile inside the thick slab, and simultaneously realize a high front-to-back ratio and low input return loss. Guidelines for an initial Yagi–Uda slot-array design are as follows:

1) driver slot length L_{dr} = first resonance length in slot;
2) reflector slot length $L_r = 1.05L_{dr}$;
3) director slot length $L_{di} = 0.9L_{dr}$;
4) element spacing $d_d = d_r = \lambda_{\rm SW}/4$ where $\lambda_{\rm SW}$ is the wavelength of the dominant TM surface-wave mode in the slab;
5) slot width = 1/10 of slot length;
6) feed-line offset $d_o = L_{dr}/10$;
7) open-stub length = $\lambda_{MS}/4$ where λ_{MS} is the wavelength in the microstrip feed line.
8) slab thickness is such that $f_o = 0.9f_c$ where f_o is the operating frequency and f_c is the cutoff frequency of the second-order TM surface-wave mode.

Guidelines 1)–4) were obtained from [14], where efficient excitation of an image line by a waveguide-fed Yagi–Uda slot-array antenna was reported. An initial estimate for the driven slot length for the antenna, shown in Fig. 2, was $L_{dr} = \lambda_{\rm SW}/2$. Offset feeding of the slot is required for matching to the 50-Ω feed line since the slot has very high input impedance when fed at its center. Coupling into the DSBW substrate was maximized by choosing the thickness to be such that the center operating frequency corresponds to 90% of the cutoff frequency of the second-order TM mode; slot excitation of the first-order TE mode is negligible. Material with a high dielectric constant was selected for the thin substrate to keep the design compatible with eventual MMIC fabrication. The microstrip substrate and slab use the same dielectric material (RT/Duroid 6010, $\epsilon_r = 10.2$), and their thicknesses are 0.02 in and 0.2 in, respectively.

Optimal performance of the surface-wave launcher was arrived at through experimental optimization of the parameters discussed above. For a good front-to-back ratio, the relative lengths and separations of the driven, director, and reflector slots must be maintained. Parameters adjusted experimentally for best impedance match were the driven slot length, feed offset position, and microstrip open-stub length. Final dimensions for the X-band prototype in [12] were obtained experimentally as follows: $L_{dr} = 0.197$ in, $d_d = d_r = 0.125$ in, and $d_o = 0.022$ in. Experimental optimization of the antenna dimensions resulted in a design with a standing-wave ratio (SWR) <2 and front-to-back ratio greater than 10 dB over a 5% bandwidth.

Element spacing for the linear antenna and amplifier arrays of Figs. 1 and 2 was chosen as small as possible, yet consistent with the Yagi–Uda antenna element dimensions. Allowing three line widths of clearance between the microstrip feed lines and the reflector slot elements results in an element spacing $d = 0.325$ in $= 0.65\lambda_{\rm SW}$. Mutual coupling was not considered in the linear array design since slots spaced end to end should not couple strongly. The number of lens elements is 10 ($N = 10$). Therefore, the lens diameter (D) is $D = Nd = 3.25$ in. Experiments with passive lenses, where the gain blocks are replaced by through lines, were conducted to determine the lens focal length. A passive lens with focal length $f = 1.4$ in had 6.7-dB insertion loss. The lens focal length to diameter ratio is $f/D = 0.43$.

Dielectric lenses were used to focus TE surface-wave modes in the 2-D quasi-optical amplifiers described in [8]–[10]. Microstrip delay lines were used to provide focusing in a 3-D power combiner [4]. Antenna arrays have been used in conjunction with delay lines to focus free-space radiation for some time. Various so-called bootlace-type lenses have been reported in the literature [15], [16]. Microstrip delay lines are used to focus TM surface waves in the slab-based amplifier in Figs. 1 and 2. Delay-line lengths for the PDQ combiner are chosen such that all paths through the lens have identical phase delay

$$l_{\rm MS} = 2\frac{\lambda_{\rm MS}}{\lambda_{\rm SW}}\left\{\sqrt{f^2+(4.5d)^2} - \sqrt{f^2+[(5.5-n)\,d]^2}\right\}. \tag{1}$$

$l_{\rm MS}$ = microstrip delay-line length, $n = 1, 2, \cdots, 10$, lens edges correspond to $n = 1$ and $n = 10$.

An advantage of the PDQ combiner is that time-delay lines can be accommodated since the antenna arrays are linear. Unlimited freedom exists in the direction orthogonal to the antenna arrays. Planar antenna arrays are used in 3-D approaches and time-delay lines cannot be incorporated, except for very small arrays, as the element spacing is constrained in a 2-D sense in order to avoid grating lobe problems. The delay lines for the PDQ discussed here are not true time-delay lines due to the fact that microstrip transmission lines and surface waves are dispersive. However, microstrip transmission lines and surface waves propagating along thick dielectric slabs have nearly linear phase versus frequency response. Therefore, the PDQ amplifier should have good group-delay performance over a limited frequency range.

III. Amplifier Measured Data

Gain of the PDQ amplifier was measured from the feed-element microstrip line to the collector-element microstrip line. Microstrip-to-coaxial SMA connectors were used to interface with a network analyzer. Measured peak gain was 11 dB at 8.25 GHz with a 3-dB bandwidth of 0.65 GHz (see Fig. 4). With no bias, the gain dropped below -30 dB over the entire frequency range measured. Peak response of a passive lens was -6.7 dB. The passive lens has through lines instead of gain blocks. Difference in peak response between the active lens and passive lens is 17.7 dB, close to the 18-dB gain of two cascaded gain blocks. Gain bandwidth of the PDQ amplifier closely matches the Yagi–Uda slot-array return-loss bandwidth (see Fig. 5). Output power at 8.25 GHz plotted against input power is shown in Fig. 6. Output power at 1-dB gain compression is 16 dBm. Phase response was nearly a linear function of frequency over the PDQ amplifier passband yielding constant group delay (see Fig. 7) and demonstrates the time-delay nature of the microstrip delay lines.

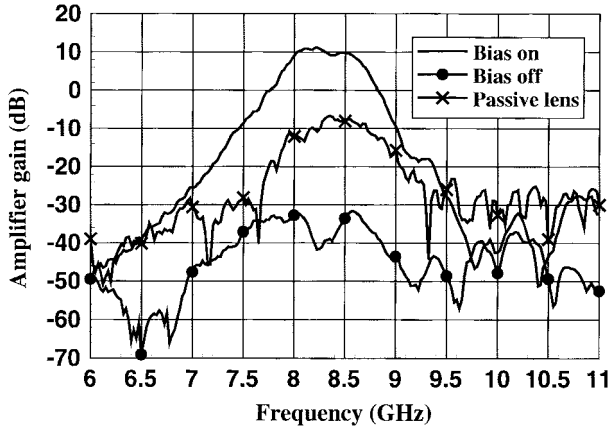

Fig. 4. Slab–beam lens amplifier gain versus frequency. The peak is 11 dB at 8.25 GHz. The 3-dB gain bandwidth is 0.65 GHz. Insertion loss of a passive lens is included for reference.

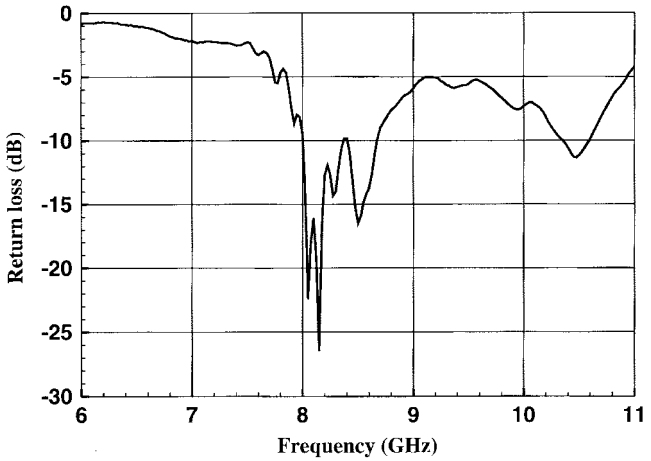

Fig. 5. Yagi–Uda slot-array input return loss versus frequency. Return loss is better than -10 dB over a 0.68-GHz bandwidth centered at 8.3 GHz. The antenna element passband matches that of the slab–beam lens amplifier (see Fig. 4).

Efficiency of the Yagi–Uda slot-array antenna can be estimated from the insertion loss (6.7 dB) measured for the passive lens. Measured microstrip line attenuation was 0.3 dB/in. Average microstrip line length from the combiner input to output is 8.0 in. Microstrip transmission-line losses are 2.4 dB (8.0 in $\times$ 0.3 dB/in). Surface-wave attenuation of the TM mode in the dielectric slab was computed as 0.15 dB/in using the method described in [19]. Loss due to the dielectric material ($\epsilon_r = 10.2, \tan\delta = 0.002$) is 0.14 dB/in. Almost all of the surface-wave attenuation is due to the imperfect dielectric. Using a high-quality dielectric material would reduce the surface-wave attenuation to that due to the imperfect ground plane, 0.01 dB/in. Surface-wave attenuation loss of the passive lens is 0.5 dB (3.4 in $\times$ 0.15 dB/in). Losses due to microstrip transmission-line and surface-wave attenuation total 2.9 dB. This leaves 3.8 dB of loss due to lens spillover and phase errors, undesired radiation, mutual coupling, and input impedance mismatch. Direct measurement or calculation of each of the losses mentioned above is difficult. However, assigning all of the loss to the Yagi–Uda antenna results in a lower bound on its efficiency. A signal passing through the passive version of the PDQ amplifier encounters the Yagi–Uda antenna four times. Therefore, the loss due to a single antenna is less than $3.8\ \text{dB}/4 = 0.95$ dB and the antenna efficiency is greater than 80%. A waveguide to slab transition should have very low losses. If waveguide transitions were used to collect the lens output power, the combining efficiency would be 80%. This combining efficiency is simply the efficiency of a single Yagi–Uda slot-array antenna.

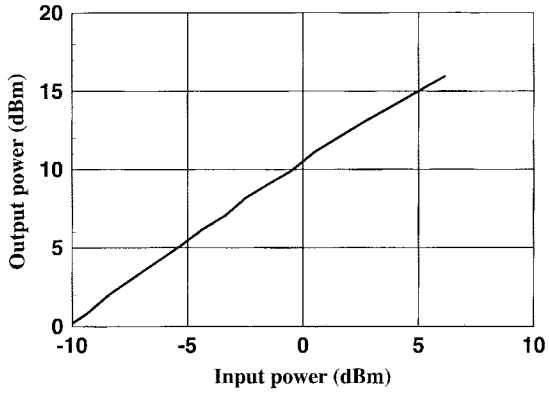

Fig. 6. Output power at 8.25 GHz plotted against input power. Output power at 1-dB gain compression is 16 dBm.

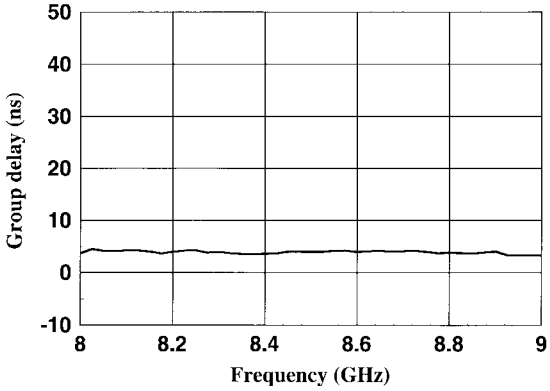

Fig. 7. Amplifier group delay as a function of frequency. Group delay is flat over the amplifier passband.

Output power of the PDQ amplifier at 8.25 GHz was 16 dBm at 1-dB gain compression. To compute the power output by the ten output gain blocks, we should add the loss due to two Yagi–Uda antennas, the surface-wave attenuation between the output array and the collector element, and the loss due to the 1.4-in-long microstrip line feeding the collector element. Therefore, the output gain blocks are producing 18.8 dBm. Typical output power at 1-dB gain compression for the Hewlett-Packard MGA-64 135 gain blocks is quoted as 12 dBm. Ten of these amplifiers driven equally would ideally yield 22 dBm. Amplitude taper on the lens causes the power to be lower. Elements in the lens center put out more power than those at the edges.

IV. Yagi–Uda Antenna Simulation and Measurement Results

Initial design and development of the Yagi–Uda slot-array antenna of Fig. 3 was accomplished using engineering rules-

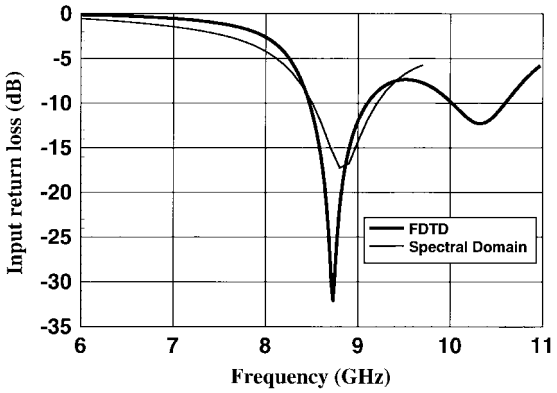

(a)

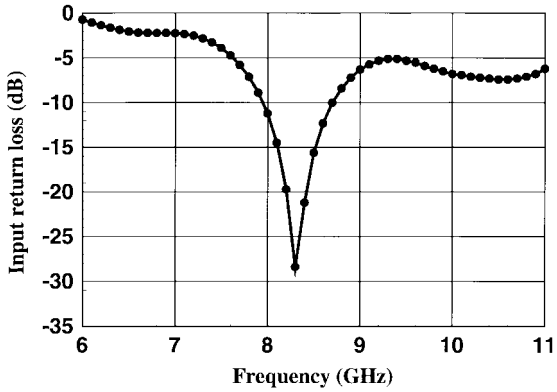

(b)

Fig. 8. (a) FDTD and spectral-domain simulated input return loss. (b) Measured results, obtained by applying gating to the data of Fig. 5, for the experimentally optimized microstrip-fed Yagi–Uda slot array.

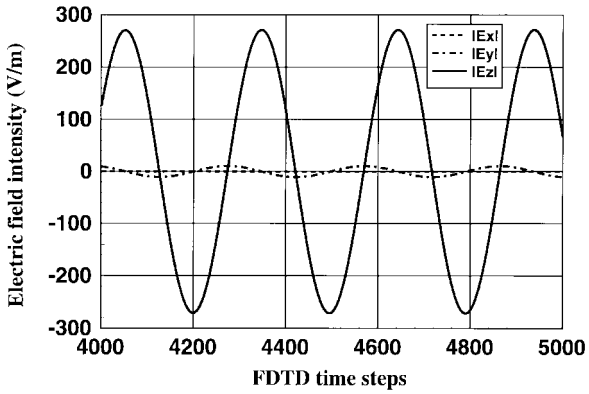

(a)

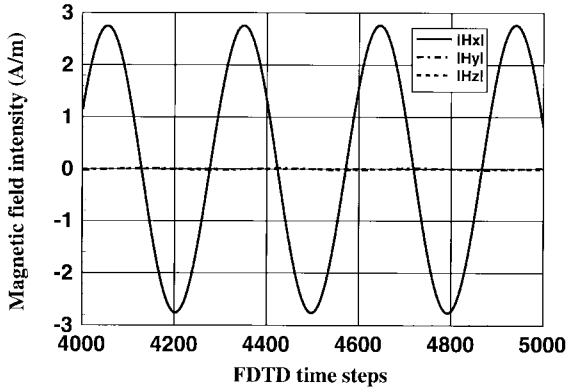

(b)

Fig. 9. Steady-state electric- and magnetic-field components at point A inside the slab waveguide (see Fig. 3), showing that only the dominant TM surface-wave mode is excited at $\phi = 90°$.

of-thumb and rapid experimental iteration. It was anticipated the antenna would be an efficient surface-wave launcher. Experimental results for the PDQ amplifier and passive lens confirmed this and provided motivation to perform further measurements and perform detailed analysis of the Yagi–Uda antenna [17], [18]. Finite-difference time-domain (FDTD) simulations were carried out for the X-band prototype in [18]. Spectral-domain and FDTD analysis results are compared with measured data in what follows. Parameters investigated include input return loss, mode purity, surface-wave field profiles, front-to-back ratio, mutual coupling, and launching efficiency.

Computed and measured input return-loss data are shown in Fig. 8. The time-domain gating feature of a Hewlett-Packard 8720 network analyzer was used to transform the return loss data, shown in Fig. 5. Multiple reflections within the low-loss dielectric slab cause the data in Fig. 5 to be rippled and are removed by using gating. Good agreement exists between the FDTD and spectral-domain simulation results. However, there is approximately 5% discrepancy with the measured resonant frequency. Over etching of the slots, the use of dielectric paste to eliminate air gaps between the slab and ground plane, and uncertainty in the thickness and dielectric constant of the slab and substrate materials are factors which could contribute to the discrepancy. FDTD and spectral-domain predicted frequency bandwidths (return loss <-10 dB) are 7.7% and 7.9%, respectively. Measured bandwidth was 8.3% and includes the effect of microstrip feed-line attenuation, which tends to improve the input return loss and increase the bandwidth.

Sinusoidal wave excitation ($f = 8.5$ GHz) was applied to the microstrip feed line and the fields radiated into the slab were simulated by the FDTD method. The steady-state time variation of all six electromagnetic-field components was recorded at point A [see Fig. 3 (b)] inside the dielectric slab and directly in front ($\phi = 90°$) of the Yagi–Uda slot array. As can be seen from the simulation results shown in Fig. 9, the vertical electric field (E_z) and transverse magnetic field (H_x) are the dominant field components excited in the slab. Therefore, the microstrip-fed Yagi–Uda slot array has successfully launched a TM-type surface wave with a high level of mode purity. The in-phase relationship between the E_z and H_x components confirms the excited surface wave is propagating along the $+y$-direction, as can be understood by the coordinate system shown in Fig. 3(a).

In order to realize a high-efficiency PDQ power combiner, the excited surface wave should be confined inside the slab waveguide and its leakage to the microstrip substrate and free space should be minimized. FDTD calculations indicate this to be the case [18]. However, FDTD computations are performed in a small volume enclosing the antenna, and one cannot be certain if the far-field profiles are the same as those

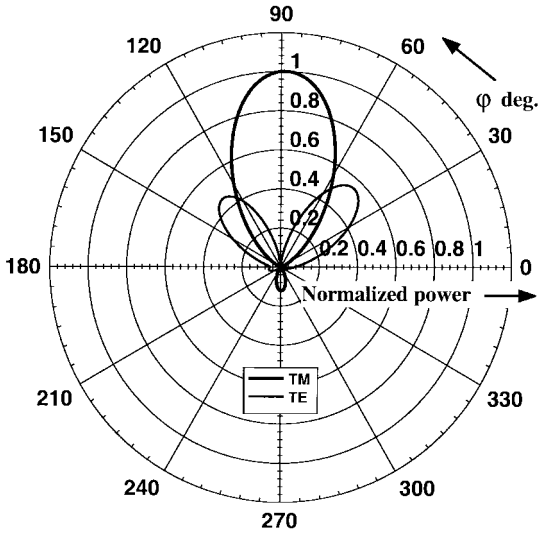

Fig. 10. Yagi–Uda slot-array antenna far-field surface-wave power patterns. Power patterns are calculated from asymptotic expressions from spectral-domain analysis. Power is normalized to unity at the TM pattern maximum at $\phi = 90°$. Vertical position for the calculations is the air side of the air–slab interface (see Fig. 3).

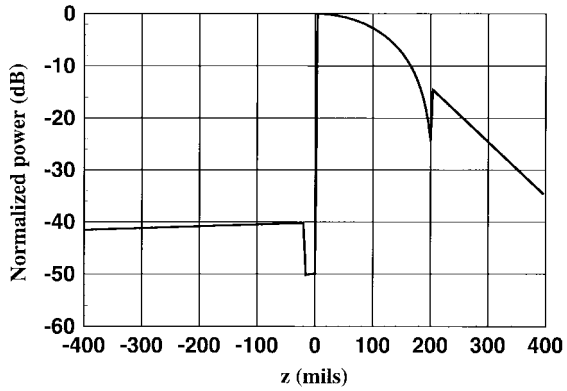

Fig. 11. Vertical TM power pattern at $\phi = 90°$. Majority of power is confined to the dielectric slab. Ground plane is at $z = 0$. Slab–air interface is at $z = 200$ mil. Dielectric substrate–air interface is at $z = -20$ mil (see Fig. 3).

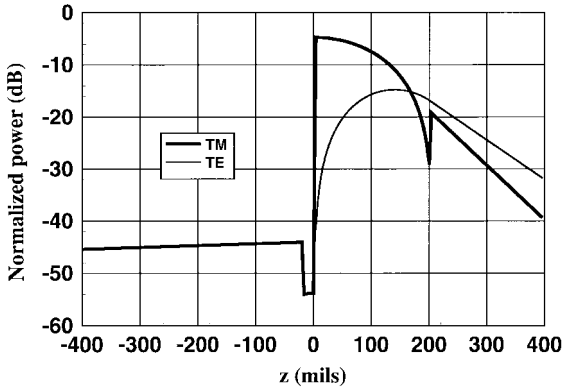

Fig. 12. Vertical TM and TE power profiles at $\phi = 43°$ (see Fig. 3). Power profiles are normalized to the TM power maximum at $\phi = 0$. Excitation of TE surface waves occurs, but is minor.

computed in the near field. Waves propagating in the slab near field may eventually give rise to far-field free-space radiation. In the spectral-domain approach, infinite slab and microstrip

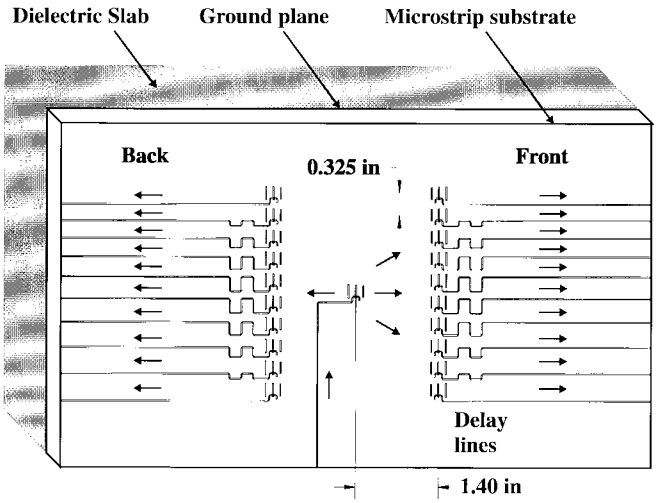

Fig. 13. Yagi–Uda slot-array antenna test circuit. Microstrip lines are on the top side of a thin substrate on top of dielectric slab. Slots are on the common ground plane.

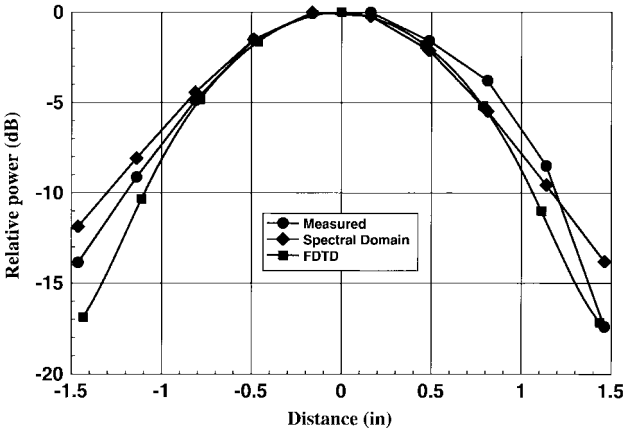

Fig. 14. FDTD and spectral-domain simulation and measured results of the Gaussian-like slab–beam profile along the transverse direction (x) in the front side of the Yagi–Uda slot array. Distance is from the center of the front array of Fig. 13.

substrates are assumed. Asymptotic expansions were carried out to obtain expressions for the far-zone surface-wave and free-space radiation. One can clearly identify and differentiate between the different modes of far-field radiation: free space, TM surface wave, and TE surface-wave radiation.

Calculated surface-wave radiation patterns of the Yagi–Uda slot-array antenna are shown plotted as a function of ϕ in Fig. 10. Vertical position for the calculations is the air region just outside the thick dielectric slab and the frequency is 8.8 GHz. The TM pattern has a well-formed forward lobe and a reduced back lobe—front-to-back ratio is 9.2 dB. TE surface-wave fields are also observed. This is expected as the slab thickness was chosen such that the second-order TM mode would be cutoff, but not the dominant first-order TM mode or the first-order TE mode. It was assumed excitation of TE modes by the antenna would be negligible. Although this is not evident from Fig. 10, further analysis to be presented later indicates minimal TE mode radiation. Asymmetry of the patterns is due the offset feeding required for matching to 50 Ω. Minor asymmetry of the TM pattern is observed. Asymmetry

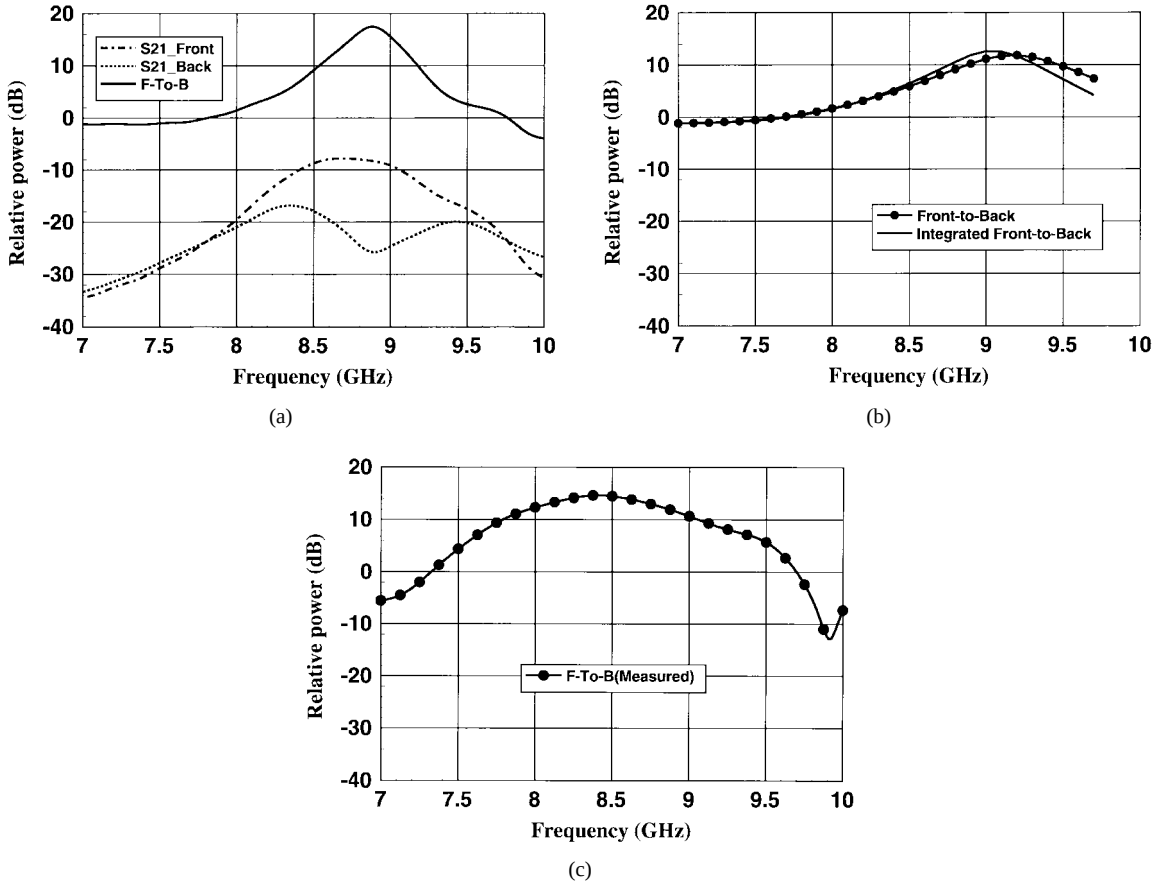

Fig. 15. (a) FDTD simulation results. (b) Spectral-domain simulation results. (c) Measured data of the front-to-back ratio of the X-band prototype Yagi–Uda slot-array antenna.

of the TE pattern is more marked, but is of no consequence since radiation of this mode is regarded as a loss.

The computed vertical TM surface-wave power profile, along the vertical (z) direction, in front of the Yagi–Uda slot array ($\phi = 90°$) is shown in Fig. 11. A null occurs in the TE surface-wave power pattern at broadside ($\phi = 90°$). Power is maximum inside the slab very near the ground plane ($z = 0^+$), and drops to -24.2 dB just before the slab–air interface. Decay in the air region is exponential as expected. A jump in power level at the slab–air interface is expected and is due the boundary condition that $D_z (D_z = \varepsilon E_z)$ be continuous across the material boundary. In the dielectric and air regions on the side of the ground plane opposite the slab, power levels are more than 40 dB below the maximum power. TM and TE vertical power profiles were computed at the TE azimuth pattern maximum ($\phi = 43°$) and are plotted in Fig. 12. TE power is zero at the ground plane and is maximum near the slab–air interface. TE modes are cutoff in the thin microstrip substrate. Maximum TE power is 15 dB below the maximum TM power. Excitation of the TE mode appears to be minimal.

The transverse field profile inside the slab should resemble that of a Gaussian beam, so that the surface wave radiated into the slab by the feed element of Fig. 1 can be properly intercepted by a linear array of Yagi–Uda elements for power combining. Surface-wave pattern measurements were conducted using the circuit of Fig. 13. Surface waves are launched primarily in the forward direction by the center element. Linear arrays are used to sample the fields radiated by the center element. Delay-line lengths were designed such that the phase measured at each array element would be identical. Measured and computed surface-wave power patterns incident on the front array of Fig. 13 are plotted in Fig. 14. Phase deviation was less than $\pm 25°$. Good agreement between theory and measurement has been observed.

The next parameter investigated was the front-to-back ratio of the Yagi–Uda slot-array antenna element. A substantial reduction in power combining efficiency will result if the surface wave is not launched in a unidirectional manner. The distance between the launching antenna and receiving linear array was 1.4 in (see Fig. 13), and both forward and backward coupling coefficients (S_{21}) were measured and simulated by FDTD. The front-to-back ratio was simply a deduction of these two coupling coefficients, and is shown in Fig. 15, together with the measured data. Front-to-back ratio peak was 17.5 dB by FDTD and 14.7 dB by experiment. Usually, the front-to-back ratio is calculated as the ratio of the power intensity directly in front of and behind the antenna. Another approach is to integrate the forward and backward radiation lobes and then take a ratio to obtain the so-called integrated front-to-back ratio. Results for both methods were computed using spectral-domain asymptotic expressions and are plotted in Fig. 15. Peak front-to-back ratios are 11.8 and 12.6 dB for the usual and integrated methods, respectively. Again, there is a slight shift in the center frequency between theory and measurement. The

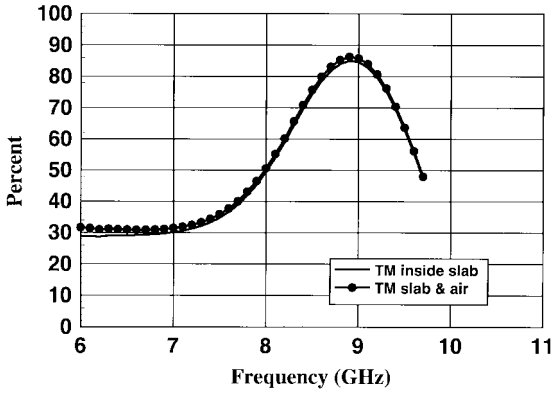

Fig. 16. Percentage of total power radiated as TM surface waves in the slab forward direction $0 < \phi < 180^\circ$. Peak percentage is 85%. Almost all the power is confined to the dielectric slab.

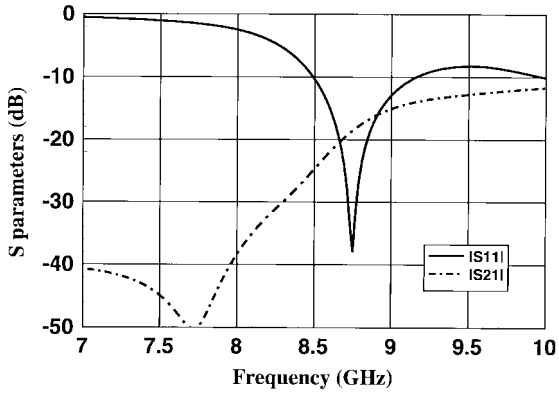

Fig. 17. FDTD simulation results of the mutual coupling (S_{21}) between two neighboring channels of Yagi–Uda slot array.

TABLE I
PERCENTAGE OF POWER RADIATED INTO VARIOUS MODES BY THE YAGI–UDA SLOT-ARRAY ANTENNA OF FIG. 3. PERCENTAGES ARE CALCULATED BY THE SPECTRAL-DOMAIN METHOD AT 8.9 GHz

Type of Radiation	Percentage of total radiation
Forward TM radiation in thick slab	85.1
Forward TM radiation in the air region adjacent to the slab	1.3
Back lobe TM radiation in thick slab	5.5
Back lobe TM radiation in the air region adjacent to the slab	0.1
Total TE radiation	7.0
Total TM radiation in the thin microstrip substrate and the adjacent air region	0.1
Total radiation to free space	0.9

good correspondence between the center frequency for peak front-to-back ratio and minimum return loss in both simulation and experiment, however, reveals that the Yagi–Uda slot array has been designed properly and works well as a unidirectional surface-wave launcher for the PDQ power combiner.

Several different types of radiation from the Yagi–Uda slot-array antenna element of Fig. 3 are possible. Forward radiation of a TM surface wave in the thick dielectric slab is the desired mode. Undesired radiation modes are as follows: backward dielectric-slab TM surface waves, dielectric-slab TE surface waves, dielectric-substrate TM surface waves, and free-space radiation. Asymptotic expressions for the radiated far fields were obtained from a spectral-domain analysis of the antenna. Integration of the expressions was performed to obtain the percentage of power radiated into each of the modes discussed above. The results are listed in Table I. Percentage of power radiated as forward TM surface waves in the thick dielectric slab is plotted as a function of frequency in Fig. 16. Maximum computed launching efficiency for the antenna is 85%.

A final concern was mutual coupling between neighboring channels of Yagi–Uda slot arrays and their possible influence on the power-combiner performance. For this purpose, the FDTD method was used to compute the coupling coefficient (S_{21}) between two neighboring Yagi–Uda slot-array antennas located in parallel, as shown in Fig. 1. The channel spacing was 0.325 in. As can be seen from the simulation results, shown in Fig. 17, the in-band (return loss < -10 dB) mutual-coupling level is below -15 dB. The input return loss is almost identical to that of an isolated Yagi–Uda slot-array antenna (see Fig. 8), indicating that mutual coupling between neighboring channels is not a major problem in the design of the PDQ power combiner.

V. CONCLUSION

A 2-D slab–beam lens amplifier has been demonstrated at X-band. The design is scaleable to millimeter wavelengths and should prove useful for efficient quasi-optical power combining of large numbers of solid-state devices. An uncommonly high peak-system gain of 11 dB at 8.25 GHz has been achieved at X-band. Amplifier 3-dB bandwidth is 0.65 GHz or 7.9%. Fabrication of the slab-based lens amplifier is compatible with planar fabrication techniques.

Comprehensive measurements and simulations of the Yagi–Uda slot array have been carried out and confirm the design philosophy of the PDQ structure proposed for millimeter-wave power combining. The FDTD method also proved itself as a very powerful and efficient computer-aided design (CAD) tool for practical design and optimization of this new type of quasi-optical structure, which is important since experimentation at millimeter wavelengths is both costly and time consuming. Measured results indicate a surface-wave launching efficiency of at least 80%. Computed efficiency is 85%.

ACKNOWLEDGMENT

The authors would like to thank Mr. M. Espiau of the UCLA Center for High Frequency Electronics, for fabrication, measurement, and trouble-shooting assistance.

REFERENCES

[1] J. W. Mink, "Quasi-optical power combining of solid-state millimeter-wave sources," *IEEE Trans. Microwave Theory Tech.*, vol. MTT-34, pp. 273–279, Feb. 1986.

[2] Z. B. Popovic, R. M. Weikle, M. Kim, and D. B. Rutledge, "A 100-MESFET planar grid oscillator," *IEEE Trans. Microwave Theory Tech.*, vol. 39, pp. 193–200, Feb. 1991.
[3] N. J. Kolias and R. C. Compton, "A monopole-probe-based quasi-optical amplifier array," *IEEE Trans. Microwave Theory Tech.*, vol. 45, pp. 1204–1207, Aug. 1997.
[4] J. S. H. Schoenberg, S. C. Bundy, and Z. B. Popovic, "Two-level power combining using a lens amplifier," *IEEE Trans. Microwave Theory Tech.*, vol. 42, pp. 2480–2485, Dec. 1994.
[5] A. Alexanian and R. A. York, "Broad-band waveguide-based spatial combiners," in *IEEE MTT-S Int. Microwave Symp. Dig.*, Denver, CO, June 1997, pp. 1139–1142.
[6] J. W. Mink and F. K. Schwering, "A hybrid dielectric slab–beam waveguide for the sub-millimeter wave region," *IEEE Trans. Microwave Theory Tech.*, vol. 41, pp. 1720–1729, Oct. 1993.
[7] F. Poegel, S. Irrgang, S. Zeisberg, A. Schuenemann, G. P. Monahan, H. Hwang, M. B. Steer, J. W. Mink, F. K. Schwering, A. Paollela, and J. Harvey, "Demonstration of an oscillating quasi-optical slab power combiner," in *IEEE MTT-S Int. Microwave Symp. Dig.*, Orlando, FL, May 1995, pp. 917–920.
[8] H. Hwang, G. P. Monahan, M. B. Steer, J. W. Mink, J. Harvey, A. Paollela, and F. K. Schwering, "A dielectric slab waveguide with four planar power amplifiers," in *IEEE MTT-S Int. Microwave Symp. Dig.*, Orlando, FL, May 1995, pp. 921–924.
[9] H. Hwang, T. W. Nuteson, M. B. Steer, J. W. Mink, J. Harvey, A. Paollela, and F. K. Schwering, "Quasi-optical power combining in a dielectric substrate," *URSI Int. Symp. Signals, Syst., Electron. Dig.*, San Francisco, CA, Oct. 1995, pp. 89–92.
[10] ———, "Two-dimensional quasi-optical power combining system performance and component design," in *IEEE MTT-S Int. Microwave Symp. Dig.*, San Francisco, CA, June 1996, pp. 927–930.
[11] A. R. Perkons and T. Itoh, "TE surface wave power combining by a planar 10-element active lens amplifier," in *IEEE MTT-S Int. Microwave Symp. Dig.*, Denver, CO, June 1997, pp. 691–694.
[12] ———, "A 10-element active lens amplifier on a dielectric slab," in *IEEE MTT-S Int. Microwave Symp. Dig.*, San Francisco, CA, June 1996, pp. 1119–1122.
[13] N. J. Kolias and R. C. Compton, "Thermal management for high-power active amplifier arrays," *IEEE Trans. Microwave Theory Tech.*, vol. 45, pp. 1204–1207, Aug. 1997.
[14] Y. Shih, J. Rivera, and T. Itoh, "Directive planar excitation of an image-guide," in *IEEE MTT-S Int. Microwave Symp. Dig.*, Los Angeles, CA, June 1981, pp. 5–7.
[15] H. Gent, "The boot lace aerial," *Royal Radar Establishment J.*, no. 40, pp. 47–58, Oct. 1957.
[16] W. Rotman and R. F. Turner, "Wide-angle microwave lens for line source applications," *IEEE Trans. Antennas Propagat.*, vol. AP-11, pp. 623–632, Nov. 1963.
[17] A. R. Perkons and T. Itoh, "Surface-wave excitation of a dielectric slab by a Yagi–Uda slot array antenna," in *26th European Microwave Conf.*, Prague, Czech Republic, Sept. 1996, pp. 625–628.
[18] Y. Qian, A. R. Perkons, and T. Itoh, "Surface-wave excitation of a dielectric slab by a Yagi–Uda slot array antenna—FDTD simulation and measurement," in *TSMMW'97 Proc.*, Shonan, Japan, July 1997.
[19] S. S. Attwood, "Surface wave propagation over a coated plane conductor," *J. Appl. Phys.*, vol. 22, pp. 504–509, Apr. 1954.

Alfred Richard Perkons was born in Anaheim, CA, on October 25, 1960. He received the B.S.E. degree in electrical engineering from the University of California at Los Angeles (UCLA), in 1983, the M.S.E.E. degree from the University of Southern California, Los Angeles, in 1987, and is currently working toward the Ph.D. degree at UCLA.

From 1983 to 1994, he worked for Rockwell International. His current research interests are the design and development of quasi-optical power combiners.

Mr. Perkons was the recipient of a Student Paper Award at the 1997 IEEE MTT International Symposium.

Yongxi Qian (S'91–M'93) was born in Shanghai, China, in 1965. He received the B.E. degree from Tsinghua University, Beijing, China, in 1987, and the M.E. and Ph.D. degrees from the University of Electro-Communications, Tokyo, Japan, in 1990 and 1993, respectively, all in electrical engineering.

From 1993 to 1996, he worked as an Assistant Professor at the University of Electro-Communications. He is currently a Post-Doctoral Researcher at the Electrical Engineering Department, University of California at Los Angeles. He has worked on various numerical techniques for microwave and millimeter-wave circuits and antennas, ultrashort electrical pulse technology, crosstalk problems in high-density MMIC's, miniature circuits for mobile communications, and millimeter-wave imaging arrays. His current research interests include high-efficiency microwave amplifiers, millimeter-wave quasi-optical power combining techniques, photonic band-gap (PBG) structures, active integrated antennas for multimedia communications and imaging arrays, as well as high-power broad-band RF photonic devices for millimeter and submillimeter-wave photodetection and photomixing. He has co-authored one book, authored a chapter for two books, and has published over 60 journal and conference papers within the above research areas.

Tatsuo Itoh (S'69–M'69–SM'74–F'82) received the Ph.D. degree in electrical engineering from the University of Illinois at Urbana-Champaign, in 1969.

From 1966 to 1976, he was with the Electrical Engineering Department, University of Illinois at Urbana-Champaign. From 1976 to 1977, he was a Senior Research Engineer in the Radio Physics Laboratory, SRI International, Menlo Park, CA. From 1977 to 1978, he was an Associate Professor at the University of Kentucky, Lexington. In 1978, he joined the faculty at The University of Texas at Austin, where he became a Professor of electrical engineering in 1981, and Director of the Electrical Engineering Research Laboratory in 1984. During the summer of 1979, he was a Guest Researcher at AEG-Telefunken, Ulm, Germany. In 1983, he was selected to hold the Hayden Head Centennial Professorship of Engineering at The University of Texas. In 1984, he was appointed Associate Chairman for Research and Planning of the Electrical and Computer Engineering Department, The University of Texas. In J1991, he joined the University of California at Los Angeles (UCLA), as Professor of electrical engineering and Holder of the TRW Endowed Chair in Microwave and Millimeter Wave Electronics. He is currently Director of Joint Services Electronics Program (JSEP), and Director of the Multidisciplinary University Research Initiative (MURI) program at UCLA. He was an Honorary Visiting Professor at Nanjin Institute of Technology, China, and at the Japan Defense Academy. In 1994, he was appointed as Adjunct Research Officer for the Communications Research Laboratory, Ministry of Post and Telecommunication, Japan. He currently holds a Visiting Professorship at the University of Leeds, Leeds, U.K. He was the chairman of USNC/URSI Commission D (1988–1990), the vice chairman of Commission D of the International URSI (1991–1993), and is currently chairman of the same Commission. He serves on advisory boards and committees of a number of organizations including the National Research Council and the Institute of Mobile and Satellite Communication, Germany.

Dr. Itoh is an Honorary Life Member of the IEEE Microwave Theory and Techniques Society, and a member of the Institute of Electronics and Communication Engineers (IEICE), Japan, and Commissions B and D of USNC/URSI. He has served as the editor of IEEE TRANSACTIONS ON MICROWAVE THEORY AND TECHNIQUES (1983–1985). He serves on the Administrative Committee of IEEE Microwave Theory and Techniques Society. He was Vice President of the Microwave Theory and Techniques Society in 1989 and President in 1990. He was the Editor-in-Chief of IEEE MICROWAVE AND GUIDED WAVE LETTERS (1991–1994).